# A SOUTHERN HEMISPHERE CASE STUDY WITH TIROS I DATA

LESTER F. HUBERT

Meteorological Satellite Laboratory, U.S. Weather Bureau, Washington, D.C.

[Manuscript received March 24, 1961; revised April 24, 1961]

## ABSTRACT

On April 28, 1960, TIROS I obtained pictures of an exceedingly sharp-edged cloud deck over the Pacific Ocean west of Chile, of cirrus associated with the jet stream on the west coast of South America, and of a mature cyclone in the central South Atlantic. Surface, upper-air, and cross section analyses are presented and compared with pictured cloud features.

Because of the wide spacing of the data, the locations of double jet streams had to be deduced by examining the horizontal temperature gradients associated with Northern Hemisphere jets and assuming that the same general relation holds in the Southern Hemisphere.

An operational surface analysis is shown to be inconsistent with the pictured data in the oceanic region where the analysis was based on a single ship report. A modification of the analysis is suggested to illustrate the potential of meteorological satellite data in data-sparse regions.

## 1. INTRODUCTION

TIROS I, the meteorological satellite launched on April 1, 1960, photographed interesting cloud patterns over many parts of the earth. From about mid-April until early May 1960 its camera orientation changed in such a manner that pictures of the Southern Hemisphere were obtained. Near the end of April some unusually interesting pictures showed what appeared to be cirrus clouds streaming off the eastern coast of Argentina. Cirrus patterns have been studied in relation to the jet stream in the Northern Hemisphere so these pictures provided an attractive case for comparison. In addition to the cirrus clouds were a sharp-edged cloud deck off the Pacific coast of South America and the classical spiral cloud pattern of a cyclone in the Atlantic east of South America. In order to examine the several interesting features of this sequence, upper-air and surface observations were obtained for a comparison between the standard meteorological data and the picture data.

The Director of the Argentina Servicio Meteorologico kindly furnished plotted and analyzed maps from their files along with some tabulated upper-air data. All observations so collected have been plotted and reanalyzed. There is little difference between the common features of the upper-air analysis furnished by the Argentina Meteorological Service and that shown here—the changes are mainly details added by incorporating the results of the cross-section analysis.

Two versions of the surface analysis are shown—the first is a copy of the operational analysis made by the Argentinian meteorologists (the oceanic portion of which is done on the basis of a single ship report), the second is modified on the basis of picture data. The purpose of the latter is to illustrate how satellite data provide invaluable information where no standard observations are available.

## 2. PICTURE DATA

Figures 1 through 6 are individual frames on which have been superimposed grids of latitude and longitude, while figure 7 is a schematic nephanalysis showing the major features. In the latter figure the picture outlines are shown with shading inside those boundaries to represent cloudiness. Inspection of the pictures will show that little can be seen near the horizon; consequently the useful part of each picture does not actually extend all the way to the horizon boundaries shown on figure 7. The various cloud patterns are described here briefly for comparison with the nephanalysis, but will be referred to again in more detail in connection with the meteorological analysis, and the analysis superimposed on the pictures will also be deferred to a later section.

Figure 1, viewing toward the western horizon, shows a sharp cloud edge in the Pacific 52° to 48° S. between a stratus deck and cumuliform clouds to the south. The sharp edge of the stratus in the left foreground is along the Andes Mountains, showing the western slopes cloudy and the eastern slopes clear. The breaks in the stratus deck near 40° S. in the Pacific correspond to the limb of the Pacific anticyclone.

Figure 2 shows a bright band across the middle of the picture which is probably cirrus and middle clouds. The stratus clouds on the west coast and the clear downslope area are again visible.

Figures 3 and 4 show the region with few scattered clouds from 40° to 50° W. longitude that is probably associated with a pressure ridge in the low troposphere.

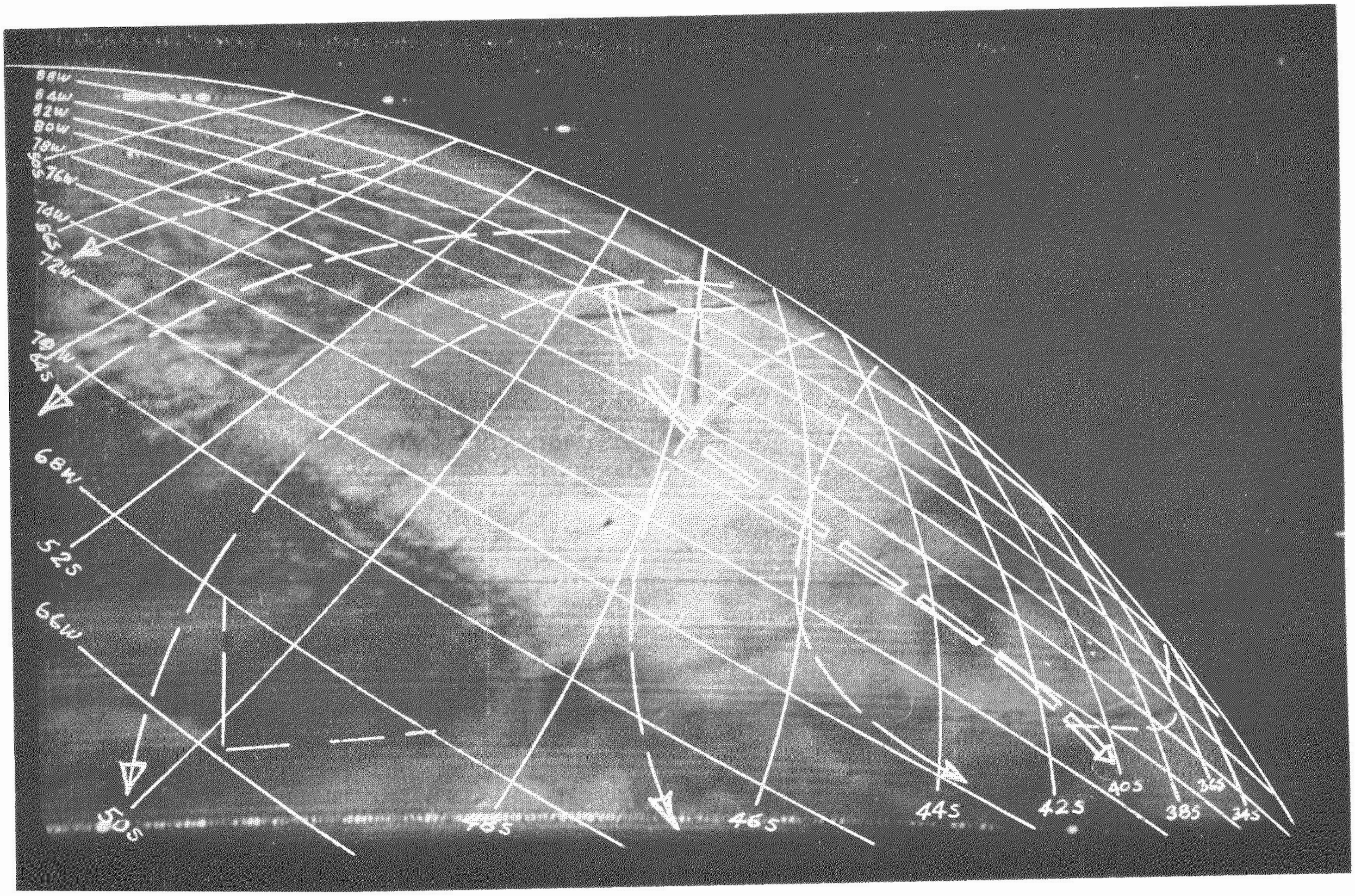


FIGURE 1.—TIROS picture toward the west *from* above Argentina. Superimposed broken lines are mean streamlines for 700–500-mb. layer; doubled broken line is jet stream axis. 1600 GMT, April 28, 1960.

Figure 5 is a view of the edge of the cyclone where a dry cool air mass has circulated toward the north around the center which is at 17° W.

Figure 6 is nicely centered on the cyclone and shows the dry air completely around the northern (equatorial) side of the cyclone. Of particular interest in this picture are the clouds standing above the lower cloud undercast, near the storm center. The shadows that appear along the eastern edge of each cloud make it clear that these are well above the lower cloud deck and have the appearance of cumulonimbus towers. However, since these elevated features are 30 to 60 miles long, they must represent a combination of cumulus towers and sheared-off cirrus nothus and perhaps some middle clouds.

## 3. METEOROLOGICAL ANALYSIS

One purpose of this investigation was to determine the location of the jet stream in the pictured area in order to associate it with the cloud features. Data for 1200 GMT April 28 and 29, 1960 were analyzed, but only analyses for April 28, corresponding to the picture time, are shown.

A space cross section approximately normal to the jet in the pictured area proved to be the critical analytical tool for this purpose. The section extended some 1500 n. mi. from northwest to southeast, but incorporated data from only three stations.

In order to estimate the proximity of the jet stream axis to a given station, the horizontal gradient of potential temperature in the various atmospheric layers was computed from 14 winter cases studied by Palmén and Newton [1] and for four autumn cases assembled for this study, all in the Northern Hemisphere. The latter limited sample was computed only for the purpose of estimating any differences that might exist between winter and autumn gradients near and beneath the jet—no claim for statistical significance is made.

The potential temperature gradients shown in figure 8 were derived as follows: temperature gradients (°C. per 60 n. mi.) for various pressure surfaces were measured

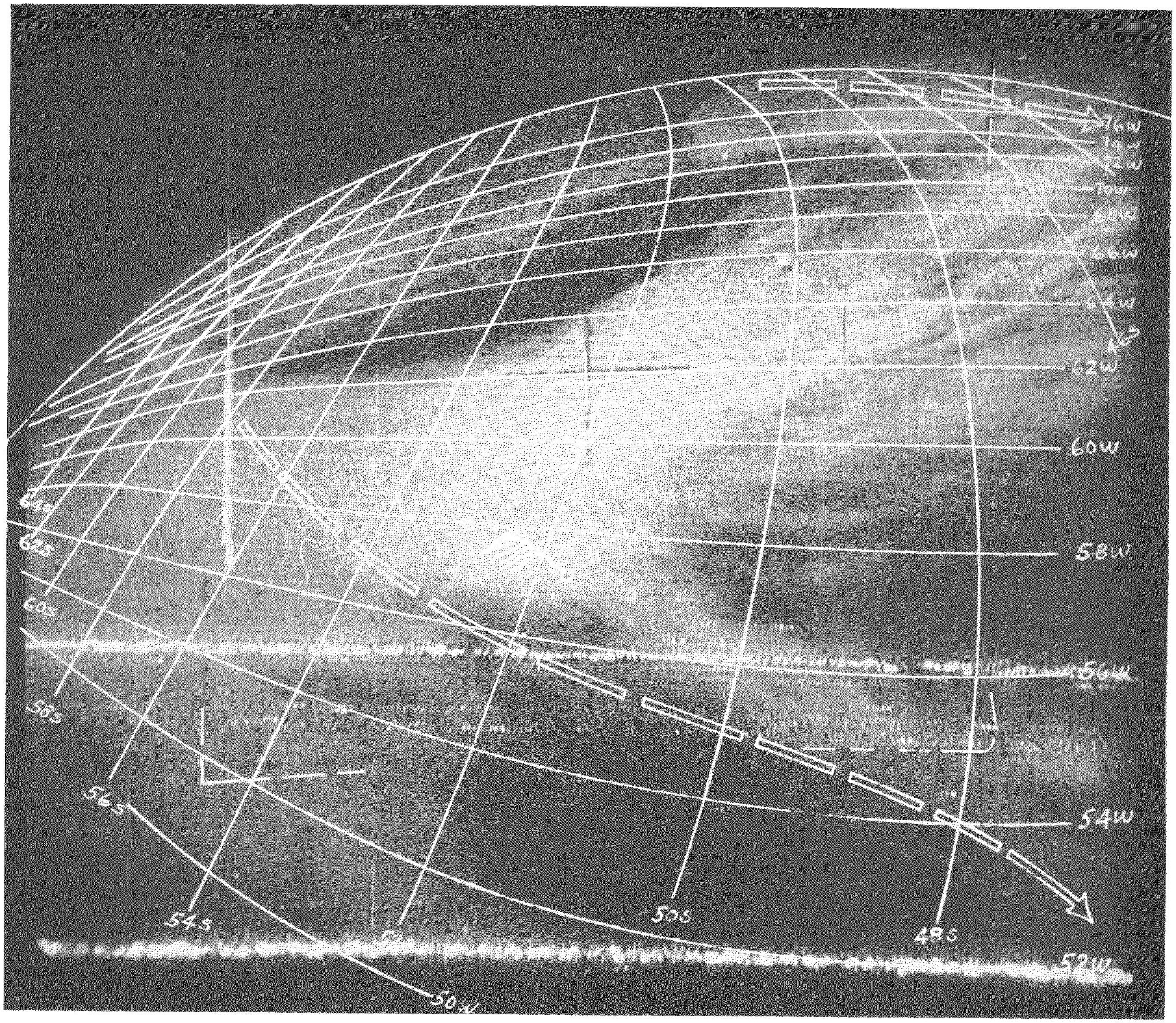


FIGURE 2.—TIROS picture over South Atlantic with South America on horizon. Doubled broken line represents jet stream axis; 200-mb. wind shown from Stanley, Falkland Islands. 1600 GMT, April 28, 1960.

from the mean cross sections of the Northern Hemisphere jets mentioned above. The potential temperature gradients were then approximated by application of equation (1):

$$\left.\frac{\partial \theta}{\partial n}\right)_p = \left.\frac{\partial}{\partial n}\right)_p \left[T\left(\frac{1000}{p}\right)^{\kappa}\right] = \frac{\theta}{T}\frac{\partial T}{\partial n} \tag{1}$$

where the subscript $p$ means differentiation at constant pressure, $T$ is temperature, $\theta$ is potential temperature, $n$ is horizontal space coordinate parallel to the pressure gradient, $p$ is pressure in millibars, $\kappa$ is $R/c_p$, the universal gas constant $R$ divided by specific heat of air $c_p$.

Reference to figure 8 shows that the potential temperature gradient maximum is nearly 4° C. per 60 n. mi. The maximum gradient near 700 mb. for the winter cases and near 400 mb. for the autumn cases reflects the intense thermal gradient of frontal regions in the low troposphere during winter contrasted to the maximum gradient occurring high in the troposphere during the warmer season. The feature used here is the value of gradient 100

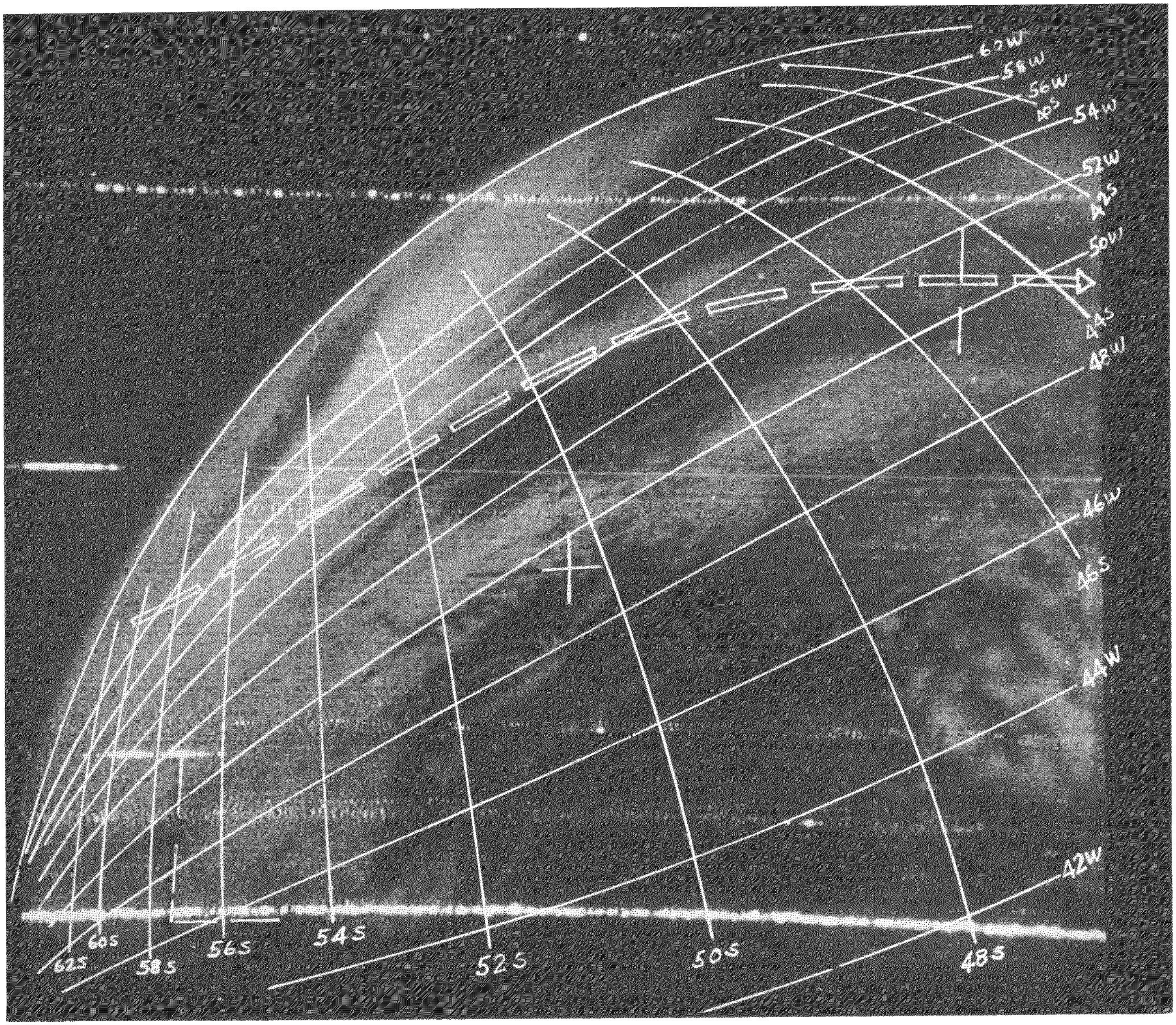


FIGURE 3.—TIROS picture of high pressure area in South Atlantic. Doubled broken line represents jet axis. 1600 GMT, April 28, 1960.

to 200 miles from the jet axis. In both autumn and winter the gradient of 2.0° C. per 60 n. mi. exists no more than 150 to 200 n. mi. from the jet axis and it is this fact that will be applied to the situation under investigation here.

Figure 9 is the space cross section for 1200 GMT April 28, 1960. The line of this section is shown on the 300-mb. map, figure 10, running from Puerto Montt, Chile (41.5° S., 72.8° W.), through Stanley, Falkland Islands (51.7° S., 57.9° W.), to the Naval Observatory at Orcadas, South Orkney Islands (60.7° S., 44.7° W.). The section is plotted with standard radiosonde and wind data. In addition the potential temperatures and potential temperature gradients are shown. The latter were computed by combining the thermal wind equation with equation (1) to give,

$$\frac{\Delta\theta}{\Delta n} \approx \frac{\theta f}{g} \frac{\Delta c}{\Delta z} \tag{2}$$

where $f$ is the Coriolis parameter, $g$ is the acceleration of gravity, and $\Delta c/\Delta z$ is the vertical wind shear.

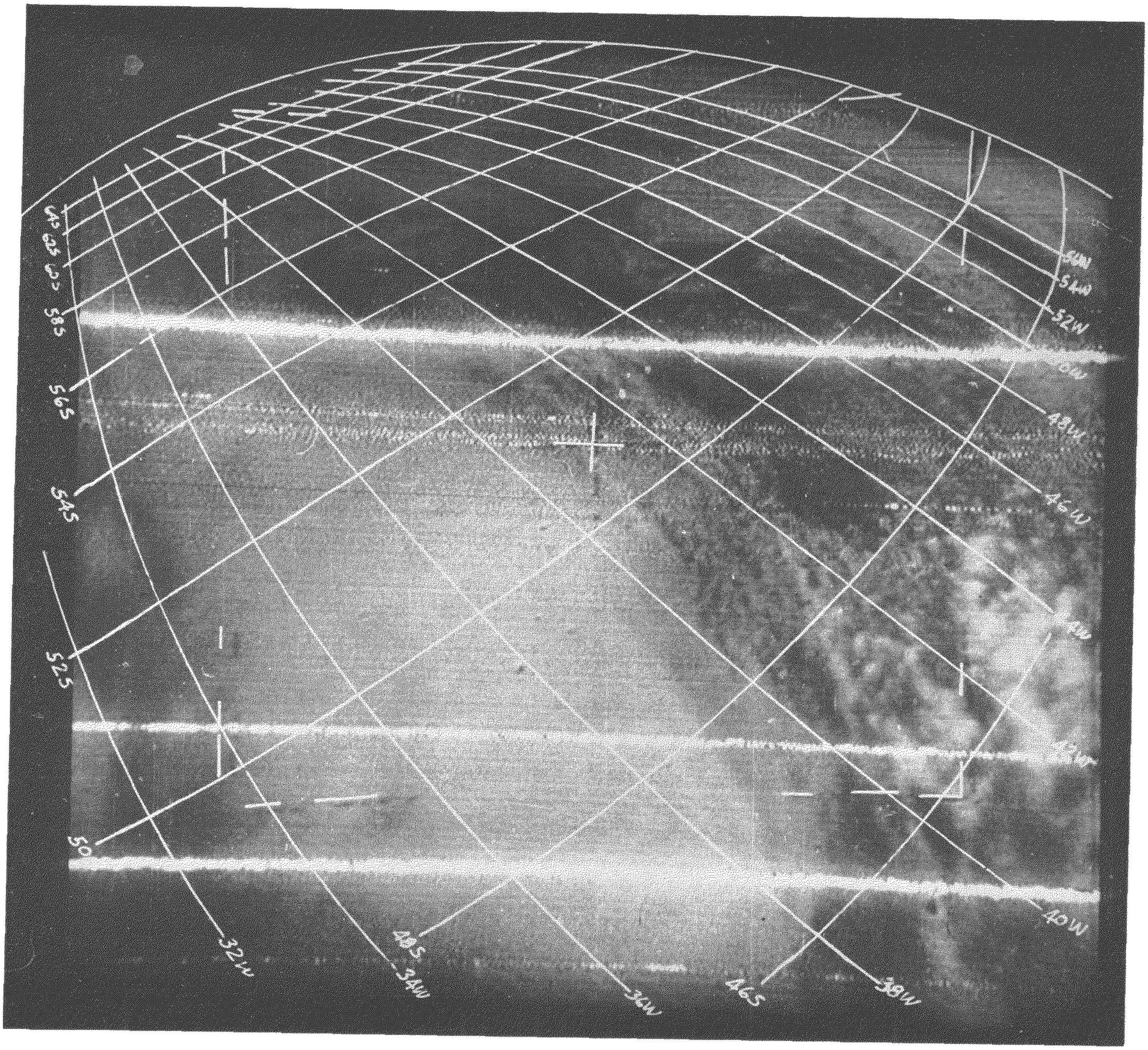


FIGURE 4.—TIROS picture showing transition area between high and low pressure areas in South Atlantic. 1600 GMT, April 28, 1960.

The vertical wind shear was computed for each atmospheric layer reported and the $\theta$-gradient was computed from equation (2) and plotted on the cross section in the same units as those used in figure 8.

Since the cross section is not strictly along the gradients or normal to the mean motion, and because of the probable existence of ageostrophic wind components, absolute consistency cannot be expected between the slope of the isentropes and the plotted gradients. Especially at the northern end of the section the shear vector and wind are not normal to the plane of the section. The analyzed slopes of the isentropes were made consistent with smaller values of $\Delta\theta/\Delta n$ (approximately 60 percent of the plotted values) in figure 9a.

In particular, shear in the layer 300 to 250 mb. over Puerto Montt implies a very large temperature gradient,*

*The gradient of 3.4° C. per 60 n. mi. immediately above a gradient of 0.5° C. per 60 n. mi. hints at an error in the wind report at 300 mb., but even if the two values are averaged, the mean value of 2.0 for the layer 400 to 250 mb. is good evidence for the implication made here.

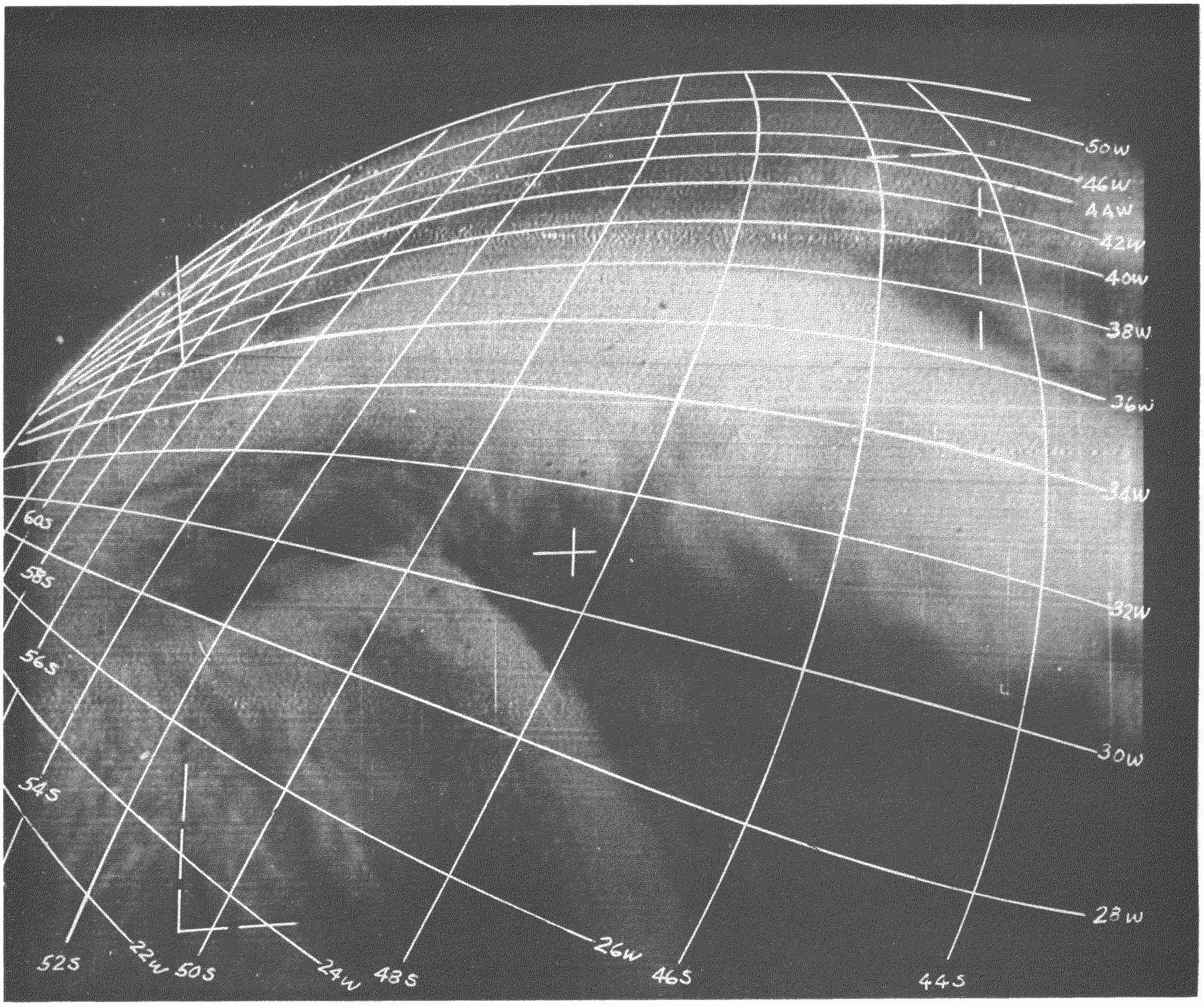


FIGURE 5.—TIROS picture showing curved cloud pattern at edge of cyclone in South Atlantic. 1600 GMT, April 28, 1960.

while the region between that station and Stanley must have a very small gradient in order to retain a reasonable pattern of isentropes. It therefore appears reasonable to postulate the existence of a jet axis northwest of Puerto Montt, and the large gradient indicates the jet axis is probably within 100 to 150 miles of the station. The data from Stanley also indicate a jet axis nearby probably within 150 miles to the southeast since the larger temperature gradients exist southeast of the station.

Figure 9b represents the same cross section but shows the isotach analysis along with lines representing the loci of maximum and minimum temperature gradients. In the low troposphere the maximum gradient is probably associated with a frontal surface and as such is shown sloping poleward. The maximum gradient near Puerto Montt, being high in the troposphere and quite similar to the jet stream gradient found at 400 mb. in figure 8b, may not be directly associated with a frontal surface.

Although it has not been included in the analysis of figure 9b, it appears that the isotach pattern between Stanley and Orcadas might have been more complex than shown here, with a primary speed maximum at the subtropical tropopause and a secondary maximum at about 350 mb., the level of the polar tropopause.

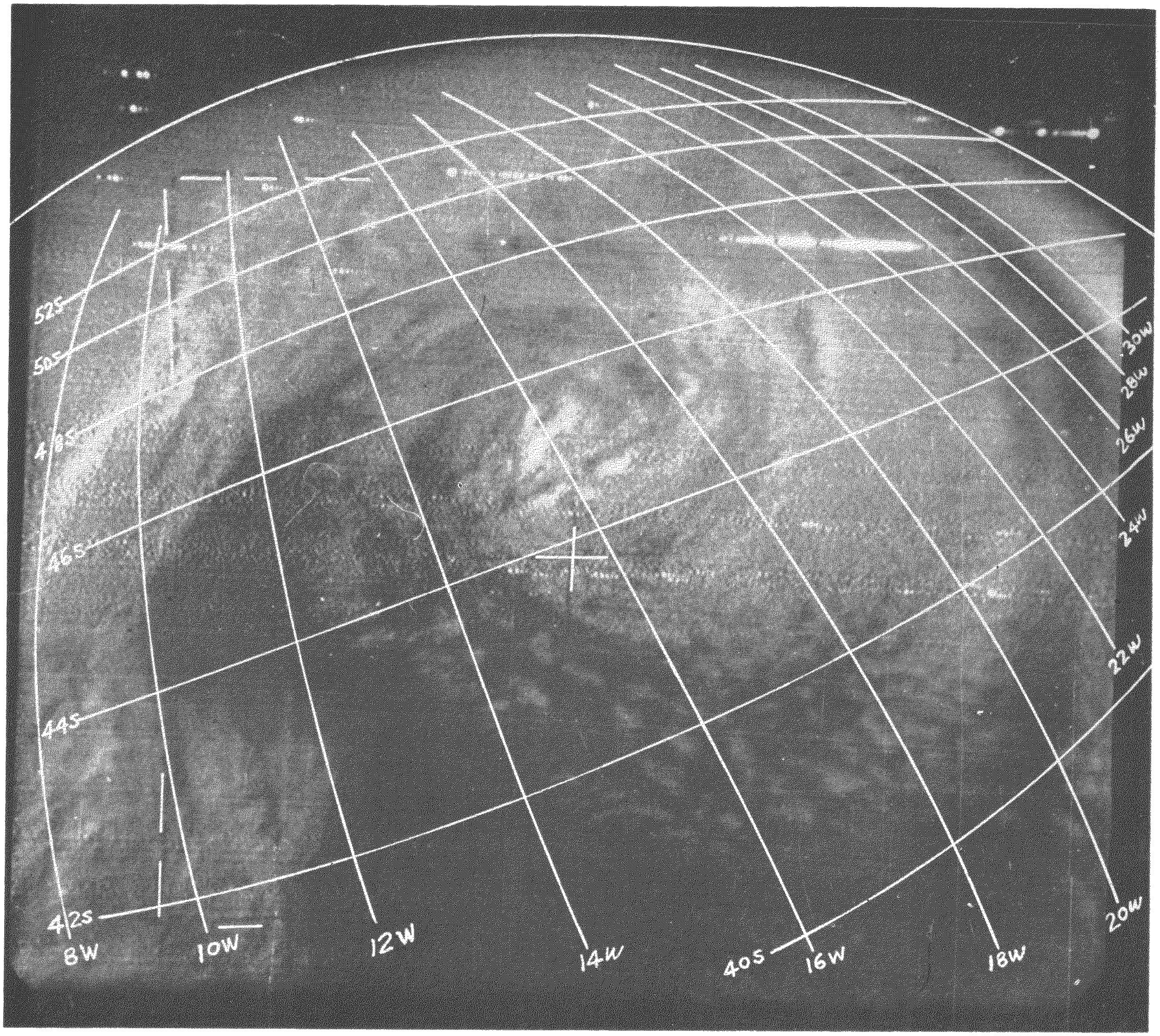


FIGURE 6.—TIROS picture showing cyclone centered at 17° W. in South Atlantic. 1600 GMT, April 28, 1960.

Figure 10 is the 300-mb. analysis for 1200 GMT April 28, 1960 on which the location of both jet axes is shown. Reference to the cross section will show that 300 mb. is not the level of maximum winds, but the general flow pattern for both jet axes is accurately represented by this level.

The closed Low was placed here because such a Low is a frequent feature of the upper flow when a double jet stream appears on Northern Hemisphere maps. The 70-kt. wind at Buenos Aires, 35° S., 59° W., lent credence to the existence of this northern jet axis, and the presence of the closed Low at this time was validated when it moved over that station 24 hours later, producing a wind of 10 kt. from the southwest.

Figure 11 shows three soundings plotted with radiosonde data also used on the cross sections. Both of the soundings over the Atlantic (Stanley and Orcadas) show relatively high moisture content to mid-troposphere, while the upper air over Puerto Montt is extremely dry and shows evidence of subsidence down to the 800-mb. level.

595485—61——4

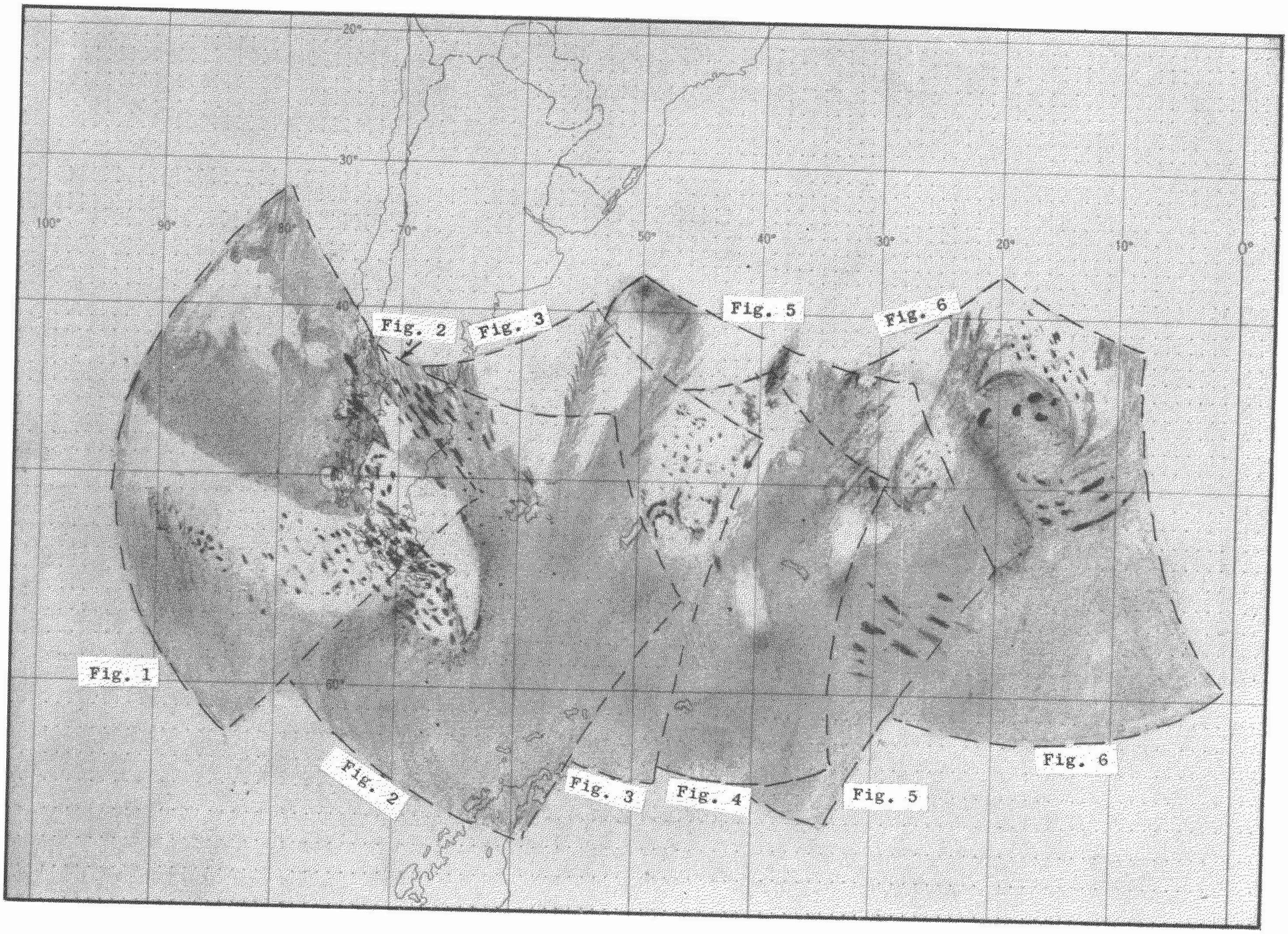


FIGURE 7.—Nephanalysis of clouds visible in TIROS pictures shown in figures 1–6. Broken outlines represent picture boundaries labeled with figures to which they refer.

Figure 12 shows a few of the surface data and analysis furnished by the Argentina Meteorological Service. Data from many continental stations have not been replotted for this illustration, but the isobaric analysis is an accurate copy of that made on April 28 in Argentina.

## 4. COMPARISON OF ANALYSES WITH PICTURE DATA

It is now possible to associate the analyzed details with the pictures. The overcast cloud deck off the west coast of Chile, shown in figure 1, is clearly below the 800-mb. level because the extreme dryness above that level at Puerto Montt could not support any cloudiness. The overcast deck that ends along the sharp line of figure 1 is a combination of fog and low stratus as shown by the data on figure 12, with the fog probably confined to the coast and the cool coastal waters. South of the 52d parallel in the Pacific the cloudiness is probably stratocumulus giving way to cumulus. The sharp division no doubt represents the boundary between two streams of air that had quite different trajectories—the warmer air from the Pacific anticyclone to the north had been stabilized as it moved over cool water, while the polar air from the south was being made unstable as it moved to lower latitudes. The stratus deck ends along the Andes Mountains in the foreground (along the 71st meridian).

Superimposed on figure 1 is the jet stream axis, representing the jet location at about 250 mb. and streamlines showing motion of the 700- to 500-mb. layer. If there were any high or middle clouds associated with the jet axis, they are invisible against the lower stratus and fog. The lower troposphere streamlines are shown here because the clouds near the Andes at 48° to 50° S. were embedded in this layer. The "bridge" of tenuous clouds at 48.5° S., 69° W. appears to be cirrus streaming across the lower cloudless area. Conditions over the pictured area of South America were unfavorable for mountain waves to occur. The sounding at Puerto Montt shows no stability in the middle and upper troposphere [2]. Probably therefore, the small cloud rows at 50° S., 70° W., lying east of the Andes, *are not* wave-produced lenticular clouds.

Figure 2 shows both jet axes transferred from figure 10 and the 200-mb. wind report from Stanley. In the upper right, the cloud area (probably middle and high clouds) 48° to 46° S. appears to have a western edge near 72° W., that is, to the cyclonic shear side of the northern jet. The cloud bands in the pattern (e.g., at 64° W.) are transverse to the wind directions at jet levels. The transverse pattern seems continuous with the bright band across the picture center which in turn lies on the equatorward side of the high-latitude (southern) jet axis. A cloud band extending from 50° S., 56° W. to 46° S., 54° W. was along the jet axis. Because of the possible error in fitting these grids to the pictures, the position of the jet axis shown here relative to this cloud band may be somewhat in error. However, this feature has the same location on an adjacent picture (not shown) and is estimated to be correctly placed within 60 to 100 miles. In any event, the main band and the finer-scale streamers are very near the jet axis, parallel to it, and probably on the equatorial side, as shown. The dark area just to the east is almost cloudless. This is associated, in the low troposphere, with a high pressure ridge containing few clouds, while at high levels there may be descent associated with the jet.

The clear area centered at 53° S., 66° W. is in the lee of the South American continent and may reflect downward motion on the lee side of the continent.

Figures 3, showing the jet axis nearer the horizon, displays more of the cloud pattern on the cyclonic shear side of the high-latitude jet. The difficulties in obtaining exact consistency between locations of the same cloud features on two different pictures are evident here when small features are compared with figure 2. Nevertheless the band of clouds and the clear areas associated with the jet axis are probably located with an accuracy of 60–100 miles and more of the general pattern near the jet can be seen. The cumuliform clouds near 47° S., 43° W. mark the transition from the high pressure ridge to the cyclone, in the low troposphere—features that are discussed below in connection with the surface analysis.

Figures 4, 5, and 6 show clouds, associated with the cyclone, which no doubt are both low and middle clouds as well as cirrus. These pictures will be used to modify the surface analysis of figure 12.

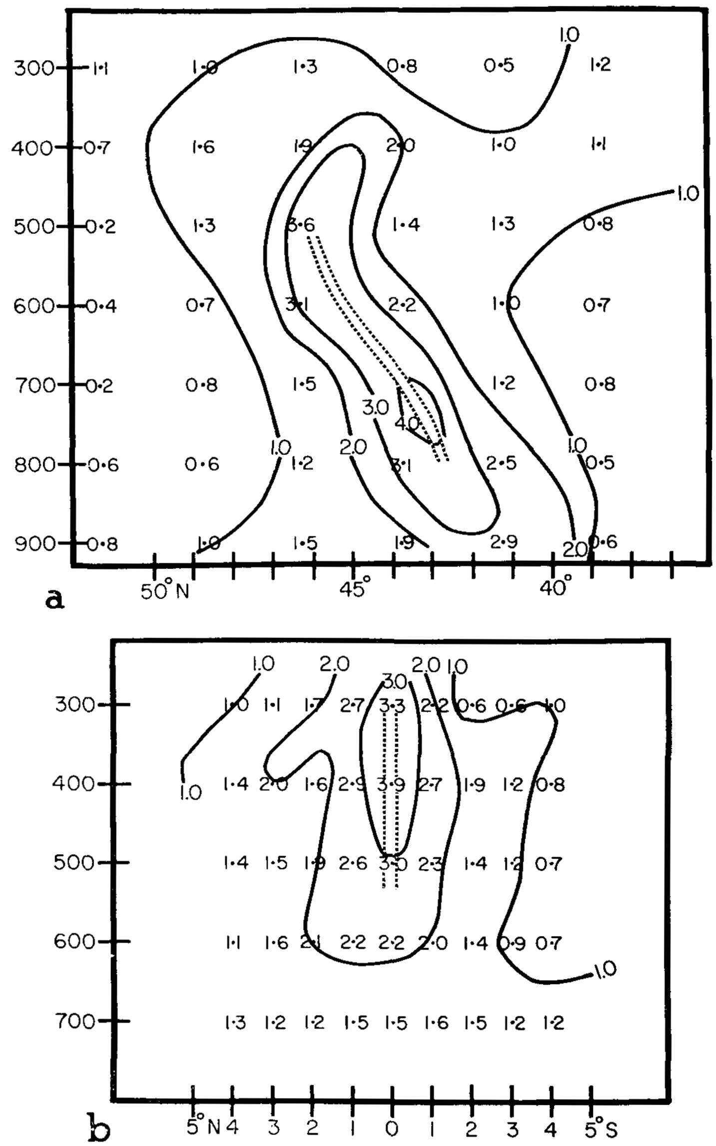


Figure 8.—Potential temperature gradients (°C. per 60 n. mi.) for Northern Hemisphere. Doubled broken line shows position of maximum gradient. (a) For 12 winter cases, (b) for 4 autumn cases; abscissa labeled in degrees of latitude north and south of jet axis.

## 5. MODIFICATION OF SURFACE ANALYSIS WITH PICTURE DATA

Comparison of the nephanalysis, figure 7, with the surface analysis, figure 12, shows that the low pressure area at 41° W. corresponds to the area covered with scattered to a few cumuliform clouds. While the Argentine analysis does not extend to 17° W., it does not seem reasonable that cyclones existed at both 41° W. and 17° W., with one showing the classical cyclonic spiral pattern and the other largely cloud-free. The surface cyclone was undoubtedly placed as shown in figure 12 on the basis of

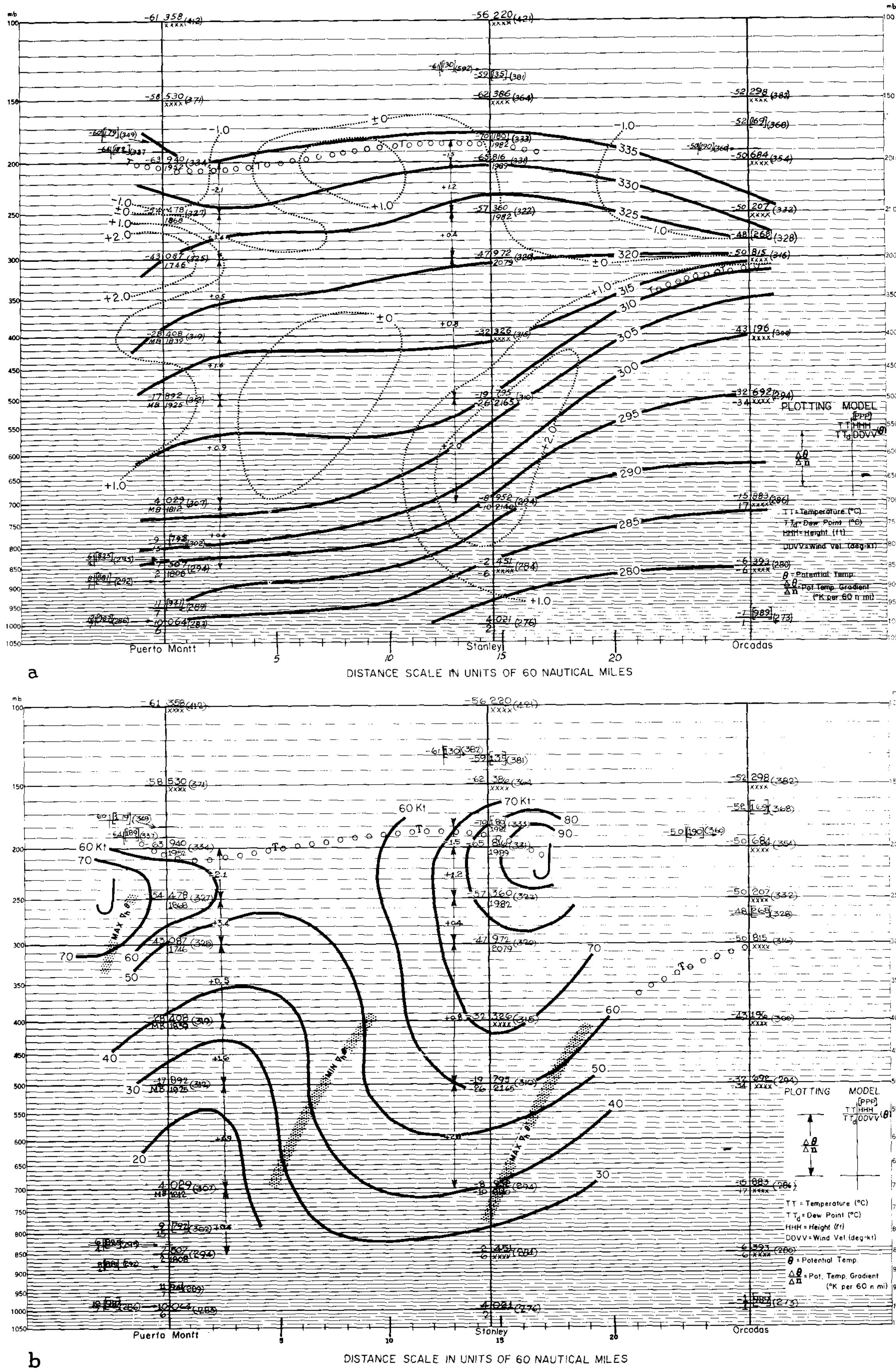


FIGURE 9.—Space cross sections for 1200 GMT, April 28, 1960; (a) showing isentropes (solid lines) and isopleths of $\Delta\theta/\Delta n$ (°C. per 60 n. mi., broken lines), and (b) showing axes of minimum and maximum temperature gradient (stippled lines) and isotachs (solid lines). Large "J" indicates best estimate of jet core location.

FIGURE 10.—300-mb. chart for 1200 GMT, April 28, 1960.

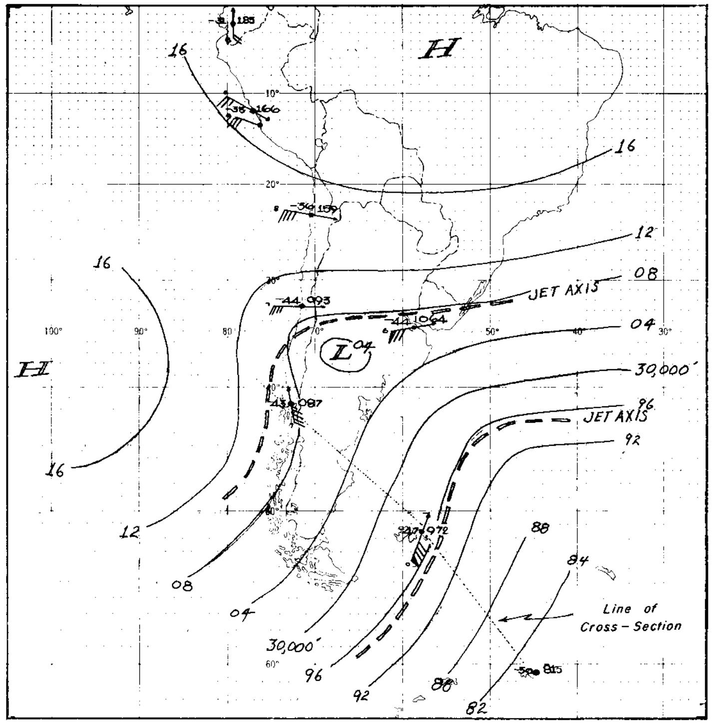


FIGURE 11.—Soundings for the three stations used in cross section (fig. 9). 1200 GMT, April 28, 1960.

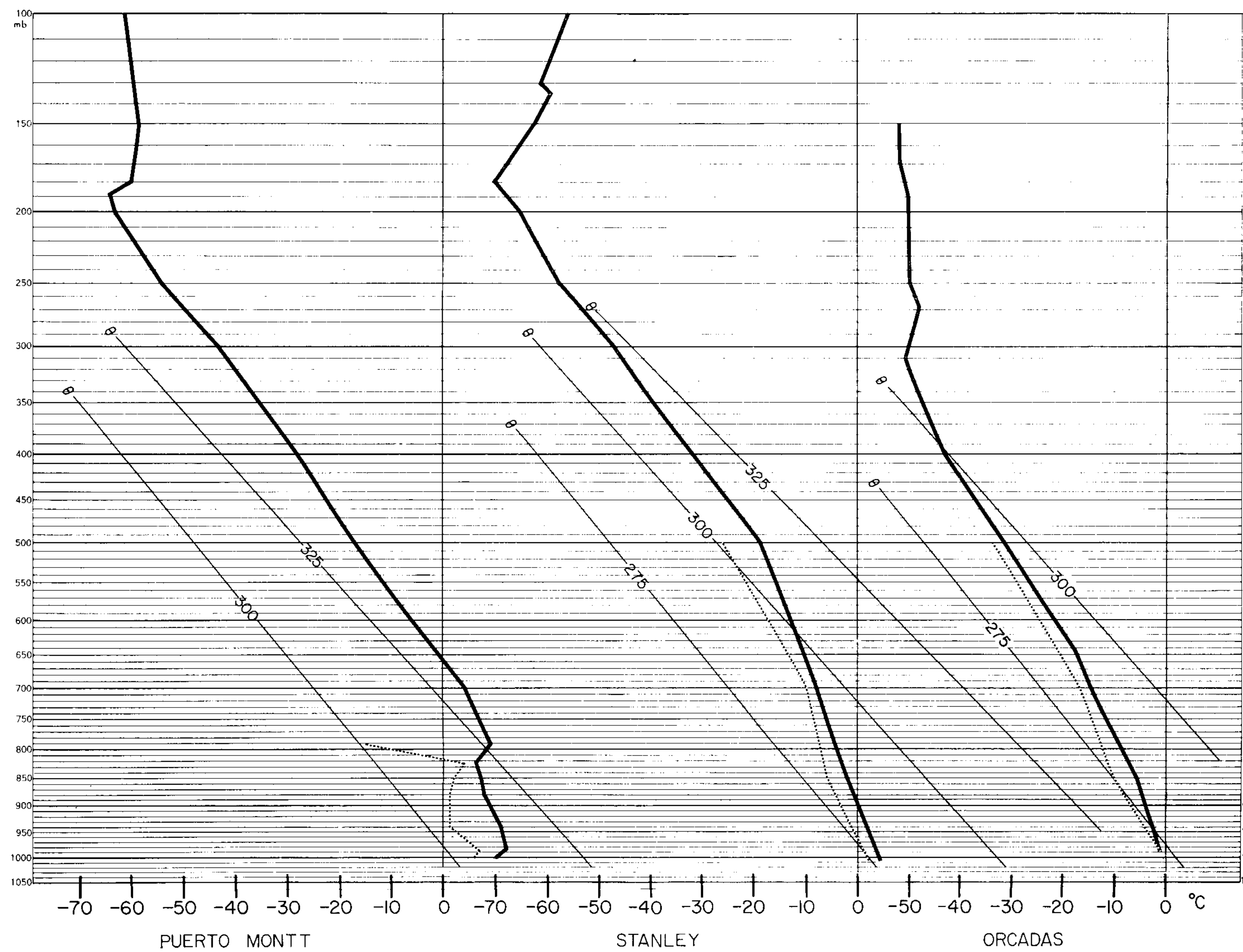

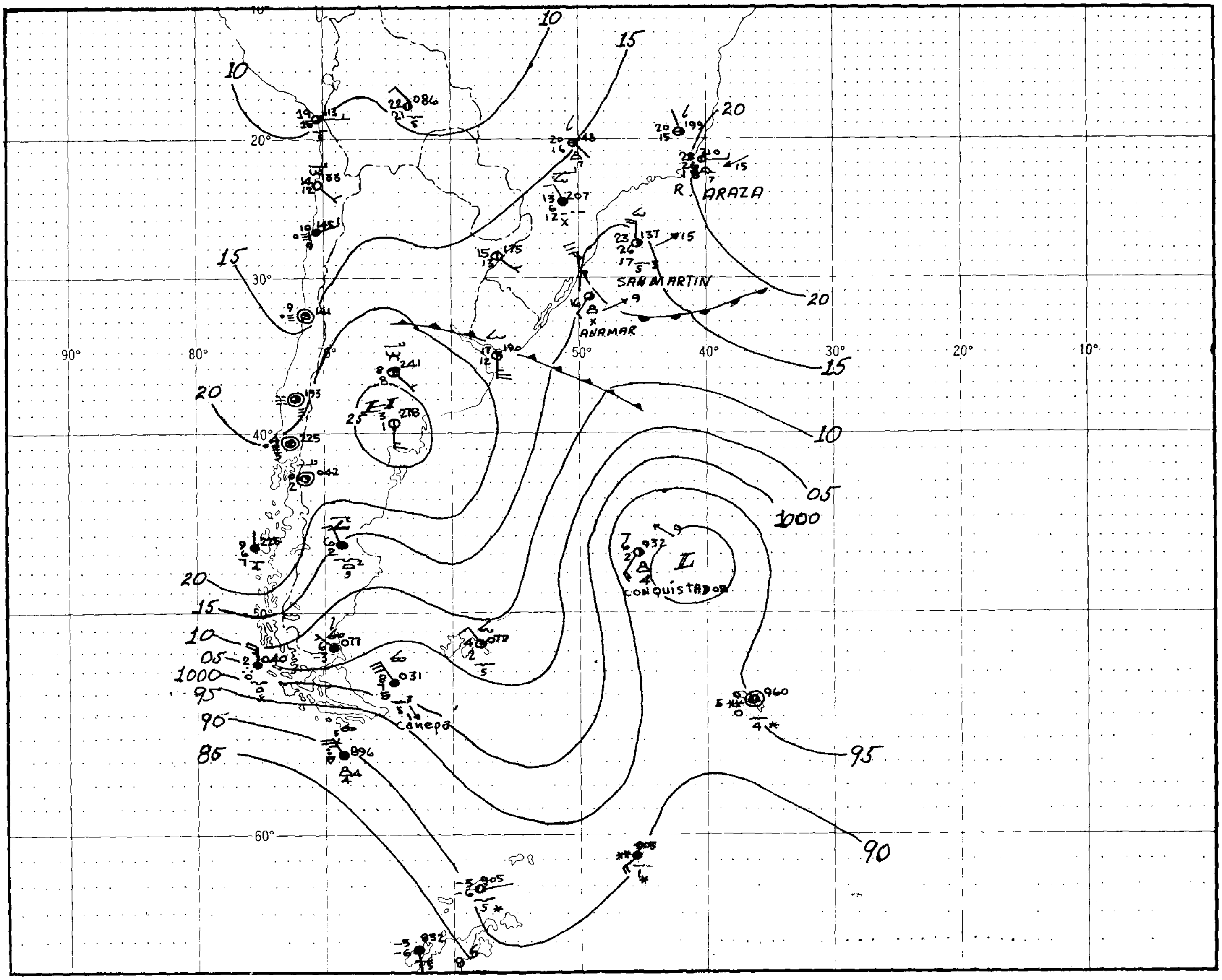


FIGURE 12.—Copy of surface data and analysis made by Argentina Meteorological Service. 1200 GMT, April 28, 1960.

the single ship report at 47° S., 45° W. In the absence of any other data the position of the Low seems entirely reasonable, but with the addition of picture data, the ship pressure appears questionable. Once doubt is thrown on the report, the analyst must decide whether the cloud type and wind speed are consistent with a deep Low so nearby. It appeared to this writer, in light of the picture data, that the ship pressure, and perhaps even the wind observation, or else the ship position, were in error. The picture data were therefore used as a basis to reanalyze the oceanic portion of the surface chart. The modified analysis is shown in figure 13.

First, the ridge line that lies on the east coast at 60° W. was extended into the zone of scattered cumuliform clouds at 50° S., 45° W. Second, an occluded cyclone (fig. 6) was located at 45° S., 17° W. That this cyclone was in the mature stage is inferred from the fact that the dry (cold) air had apparently circulated completely around the north (equatorial) side of the center and was producing a

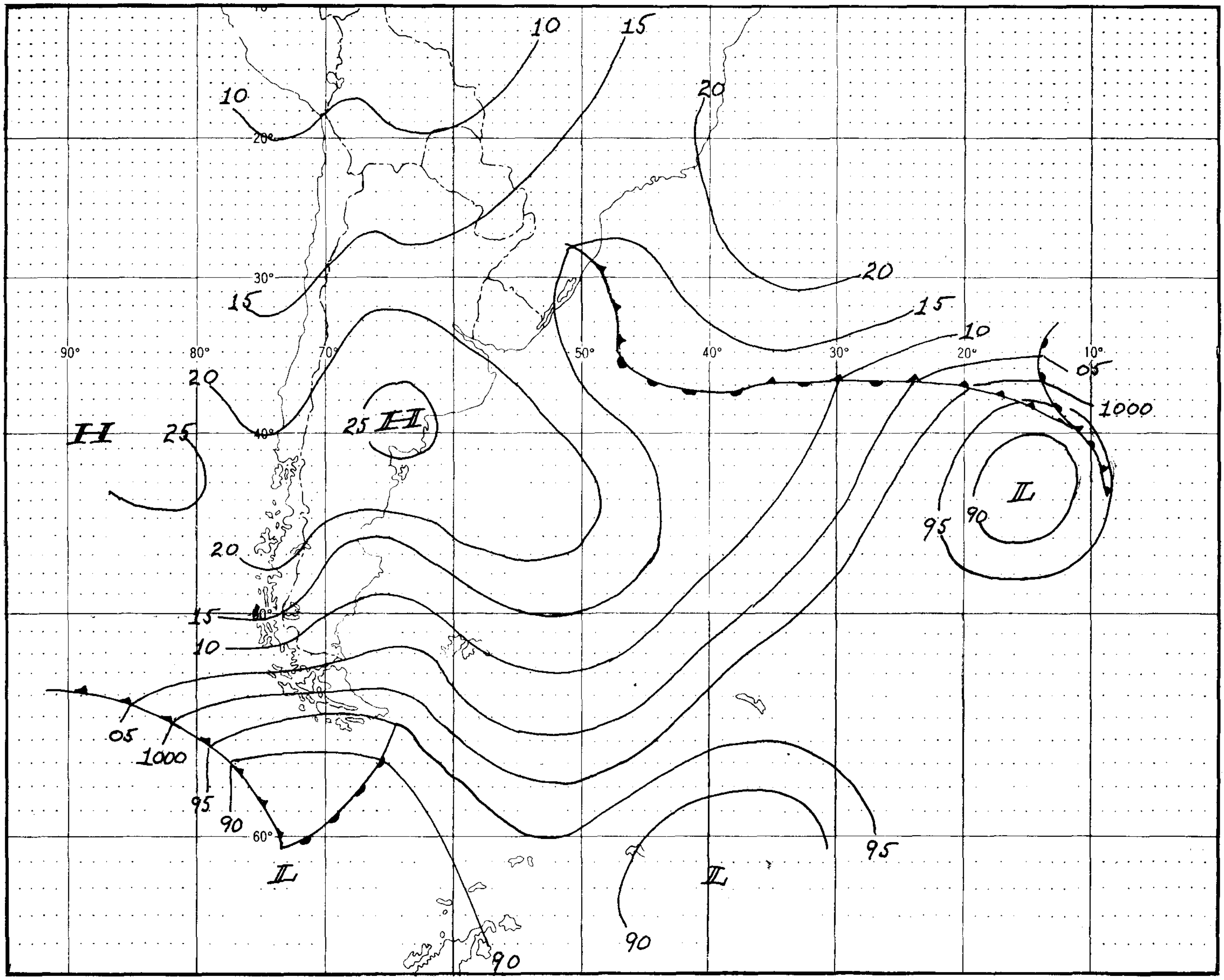


FIGURE 13.—Modification of figure 12 by use of TIROS pictures.

scattered to cloudless projection toward the center from the northeast.

Third, fog and stratus down to 52° S. along the west coast of South America indicate no front or cyclone in that immediate vicinity, but the sharp line marking the edge of the stable air implies it is a line between air masses of significantly different trajectory, and for that reason the pressure pattern southwest of South America is suggested. This portion of the analysis is of course completely outside any meteorological or picture data available at this writing and is thus little more than speculation. The cyclone in the Atlantic is, however, located with a high degree of confidence as is the ridge line extending southeastward from the continent.

## 6. CONCLUSIONS

This case study illustrates:

(1) The cloud patterns associated with cyclones and fronts are of a sufficient scale and simplicity to enable meteorologists to extract much valuable diagnostic data from satellite pictures.

(2) Cloud patterns associated with jet streams (and perhaps many other synoptic models of the upper atmosphere) are so varied and complex, that much more research must be completed before the meteorologist can exploit satellite pictures by themselves for location of the jet stream. This is true partly because the fine detail of patterns near the jet that have been documented by surface and airplane photographs are largely invisible on the currently available satellite pictures. The investigation of jet cloud patterns for satellite use must concentrate on the larger-scale distribution.

## ACKNOWLEDGMENT

The computation of the locator grids for the TIROS pictures illustrates one of the essential support functions of the Computation Section of the Meteorological Satellite Laboratory.

The work on this study has been supported by the National Aeronautics and Space Administration.

## REFERENCES

1. E. Palmén, and C. W. Newton, "A Study of the Mean Wind and Temperature Distribution in the Vicinity of the Polar Front in Winter," *Journal of Meteorology*, vol. 5, No. 5, Oct. 1948, pp. 220–226.
2. M. A. Alaka, "Aviation Aspects of Mountain Waves," World Meteorological Organization, *Technical Note No. 18*, WMO-No. 68, TP. 26, 1958, 48 pp.